Journal of Environmental Management 344 (2023) 118466

Contents lists available at ScienceDirect

Journal of Environmental Management

journal homepage: www.elsevier.com/locate/jenvman

Research article

Probabilistic assessment of failure of infiltration structures under model and parametric uncertainty

Aronne Dell'Oca [a,b], Alberto Guadagnini [b,c], Monica Riva [b,c,*]

[a] Institute of Environmental Assessment and Water Research, IDAEA-CSIC, Carrer de Jordi Girona, 18-26, 08304, Barcelona, Spain
[b] Dipartimento di Ingegneria Civile e Ambientale (DICA), Politecnico di Milano, Piazza Leonardo da Vinci 32, 20133, Milano, Italy
[c] Department of Hydrology and Atmospheric Sciences, University of Arizona, Tucson, AZ, 85721, USA

ARTICLE INFO

Keywords:
Probability of failure
Uncertainty quantification
Infiltration structure
Global sensitivity analysis
Multi-model context

ABSTRACT

We focus on the quantification of the probability of failure (PF) of an infiltration structure, of the kind that is typically employed for the implementation of low impact development strategies in urban settings. Our approach embeds various sources of uncertainty. These include (*a*) the mathematical models rendering key hydrological traits of the system and the ensuing model parametrization as well as (*b*) design variables related to the drainage structure. As such, we leverage on a rigorous multi-model Global Sensitivity Analysis framework. We consider a collection of commonly used alternative models to represent our knowledge about the conceptualization of the system functioning. Each model is characterized by a set of uncertain parameters. As an original aspect, the sensitivity metrics we consider are related to a single- and a multi-model context. The former provides information about the relative importance that model parameters conditional to the choice of a given model can have on PF. The latter yields the importance that the selection of a given model has on PF and enables one to consider at the same time all of the alternative models analyzed. We demonstrate our approach through an exemplary application focused on the preliminary design phase of infiltration structures serving a region in the northern part of Italy. Results stemming from a multi-model context suggest that the contribution arising from the adoption of a given model is key to the quantification of the degree of importance associated with each uncertain parameter.

1. Introduction

Waterlogging and/or flooding are documented to be intensified in recent years (e.g., Tellman et al., 2021 and references therein). This is mainly related to combined effects of (*i*) an increased degree of urbanization and (*ii*) climate changes (e.g., Semadeni-Davies et al., 2008; IPCC et al., 2013; Winsemius et al., 2015; Wang et al., 2018; Sohn et al., 2019; Xu et al., 2019a; Pour et al., 2020; Saurav et al., 2021; Cea and Costabile, 2022). In this context, low impact development (LID) strategies relying on infiltration (or drainage) systems are key to alleviate ensuing economic, health, environmental, and safety issues (e.g., Dietz, 2007; Todeschini et al., 2012; Qin et al., 2013; Ahiablame et al., 2013; Demuzere et al., 2014; Chaffin et al., 2016; Hu et al., 2017; Recanatesi et al., 2017; Braswell et al., 2018; Eaton, 2018; Li et al., 2019; Koc et al., 2021; Darnthamrongkul and Monzigo, 2021; Rong et al., 2022; Pumo et al., 2023).

Design and planning of LID structures is still routinely performed on the basis of best practice guidelines and upon relying on empirical and/or semi-empirical methods (e.g., Akan, 2002; Woods-Ballard et al., 2007; Bach et al., 2014) or optimization strategies (Baek et al., 2015; Ahiablame and Shakya, 2016; Wang et al., 2017; Zhu et al., 2019; Saadatpour et al., 2020; Gao et al., 2022; Li et al., 2022) while assuming a deterministic knowledge of the (surface and subsurface) system under investigation. Otherwise, it is broadly recognized that uncertainty is a critical common denominator affecting our understanding of the functioning of surface and subsurface environments and their feedbacks with anthropogenic actions (e.g., Zeng et al., 2019; Blöschl et al., 2019 and references therein). Multiple sources of uncertainties are embedded in almost all of the main elements required for the design of an infiltration structure. These include, e.g., (*i*) the intensity-duration-frequency (IDF) curve, describing the link between extreme rainfall intensity, duration, and frequency (e.g., Coles, 2001; Yeo et al., 2021); (*ii*) the hydraulic and hydrological features of the urban catchment, and (*iii*) attributes of the subsurface environment, such as, e.g., location of groundwater free

* Corresponding author. Dipartimento di Ingegneria Civile e Ambientale (DICA), Politecnico di Milano, Piazza Leonardo da Vinci 32, 20133, Milano, Italy.
E-mail address: monica.riva@polimi.it (M. Riva).

https://doi.org/10.1016/j.jenvman.2023.118466
Received 25 January 2023; Received in revised form 9 June 2023; Accepted 18 June 2023
Available online 6 July 2023

surface or aquifer conductivity (e.g., Bianchi Janetti et al., 2019 and references therein). The latter aspect is particularly relevant in shallow groundwater systems (e.g., Zhang et al., 2019).

Several studies analyze the impact of climate change on IDF curves, which are routinely adopted for the design infiltration infrastructures (e.g., Larsen et al., 2009; Wang et al., 2014; Ragno et al., 2018; Lima et al., 2018; Hosseinzadehtalaei et al., 2020; Kourtis and Tsihrintzis, 2022). Albeit literature results are not always in agreement (and may vary depending on the climate scenario and location analyzed, on the technique implemented for space-time downscaling, as well as on the duration and return period of the considered event) all of them evidence a significant increase of extreme rainfall intensities (in some cases by more than 500%). In the context of urban hydrology, Sohn et al. (2019) review the influence of climate changes on the effectiveness of LID infiltration systems, suggesting that climate variability has a stronger impact on the reduction of the overall runoff volumes than on peak flow. Recently, Busker et al. (2022) highlight benefits of incorporating weather forecasts in the operational schedule of a blue-green roof, thus enhancing the efficiency of the latter to cope with extreme rainfall events.

Together with the characteristics of the rainfall event(s), the relevance of other elements pertaining to the description of the urban catchment and to the infiltration facilities has been investigated (Todeschini et al., 2012; Zischg et al., 2018; Mei et al., 2018; Zeng et al., 2019; Yao et al., 2020). Impacts of climate change and increasing urbanization have also been considered while assessing the behavior of LID practices based on infiltration structures in urban catchments (e.g., Saurav et al., 2021). Wang et al. (2018) assess the hydrological effects and performance of LID facilities for four urban catchments (two in Singapore and two in Shezen, China) under plausible urbanization and climate change scenarios, finding that the impacts of urbanization are more severe and adverse than those of climate change. Recently, Sui and van de Ven (2023) investigated the impact of five LID implementations and three urbanization scenarios on the hydrological behavior of a half-urbanized catchment in San Antonio (USA). Notably, under extremely wet conditions, implementation of LID practices results in stacking of rural and urban sub-flows due to delay of the urban peak runoff, leading to enhanced peaks at the basin-scale.

These sets of investigations provide valuable and critical insights on functioning and ensuing impacts of infiltration structures. Otherwise, none of the above-mentioned studies relies on formal and rigorous elements of sensitivity analysis (SA; e.g., Pianosi et al., 2016; Razavi et al., 2021 and references therein) that would be key to assist to (*a*) identifying the most influential model parameters whose knowledge can improve model predictions, (*b*) enhancing our knowledge on major aspects of the dynamics of the system under investigation, and (*c*) pinpoint model parameters with limited effect, so that these could be fixed without significantly affecting model outcomes of interest. In broad terms, SA approaches can be classified according to Local and Global strategies. Local Sensitivity Analysis (LSA) techniques rely on perturbation of parameters (generally one at the time) around reference values, the ensuing SA being strongly impacted by the selected refence values. Otherwise, in a Global Sensitivity Analysis (GSA) context model parameters affected by uncertainty are typically varied (jointly) across their corresponding ranges of variability to then provide a quantification of the importance of each model parameter on the basis of indices characterizing the overall model output (or response surface). Thus, GSA is seen to yield enhanced knowledge about model functioning through a comprehensive characterization of the way uncertainty associated with each of the model parameters propagates onto a selected model output of interest and drives model behavior.

LSA and GSA have been employed to assess the sensitivity of the hydraulic and hydrological behavior of urban catchments in the presence of infiltration structures. Jia et al. (2015) rely on a LSA to assess the relevance of hydrologic model parameters on the annual runoff volume and peak flow. Locatelli et al. (2015) analyze the performance of an infiltration trench upon relying on rainfall time series from Copenhagen (Denmark) as input and conclude that soil hydraulic conductivity is one of the most influential parameters for the system functioning. Song et al. (2018) employ LSA in a decision support system assisting the design and planning of LID facilities. Xu et al. (2019b) and Dell et al. (2021) leverage on the GSA-based Morris' indices (Morris, 1991) to identify the set of influential model parameters to be then taken into account during the optimization phase of LID structures. Li et al. (2018) screen the sensitivity of three bioretention tanks upon relying on the Morris' approach and find important effects of the return period of the rainfall event and of the type and thickness of the artificial fillers on the hydraulic behavior of the three facilities. Other studies (e.g., Liu et al., 2016; Brunetti et al., 2018; Leimgruber et al., 2018) rely on a GSA approach grounded on the classical variance-based Sobol' indices (Sobol, 1993). Brunetti et al. (2018) combine surrogate modeling with a mechanistic modeling approach to simulate the hydrological and hydraulic behavior of a LID facility in the Calabria region (Italy). Their results indicate that parameters associated with the unsaturated hydraulic conductivity of the filtering layer are the most influential quantities. Leimgruber et al. (2018) assess the influence of LID design parameters on the water balance components. Madrazo-Uribeetxebarria et al. (2021) explore the way some parameters of a LID strategy based on permeable pavements control the reduction of flow volume and peak values. Floch et al. (2022) employ both Morris's and Sobol's GSA approaches to assess the sensitivity of the implementation of LID strategies in an urban catchment in Norway, while considering diverse urbanization and climate change scenarios. Hashemi and Mahjouri (2022) perform a variogram-based GSA (Razavi and Gupta, 2016) of three goodness-of-fit metrics associated with the evaluation of runoff in an urban watershed in Iran. Fatone et al. (2021) leverage on a SA merging elements of local and global SA strategies to assess the sensitivity of the hydrograph of an urban catchment in Poland with respect to the temporal distribution and intensity of the rainfall event.

As a complement to the studies illustrated above, we recall that GSA has also been employed to investigate pollution dynamics in urban catchments (e.g., Hong et al., 2019; Yang et al., 2021; Naves et al., 2020). Moreover, some studies benefit from the use of SA to enhance our level of knowledge on hydraulic and hydrological responses of urban catchments (even without necessarily focusing on the impact of LID facilities (e.g., Ballinas-González et al., 2020; Zakizadeh et al., 2022).

We remark that the formulations and approaches to SA described above are solely geared towards the evaluation of model parameters. Otherwise, they do not embed explicitly the impact of model uncertainty on target system performance metrics, which comes into play when limited knowledge leads to multiple plausible conceptual-mathematical models. As seen above, the latter source of uncertainty is typically tackled through scenario-based applications while mainly exploring parametric uncertainties within each of these. In the context of the broad area targeting modeling of urban watershed dynamics, it is recognized that the definition of the model formulation (together with its related parametrization) is generally affected by uncertainty. For example, diverse (and often competing) model formulations can be employed to describe the link between inflows and outflows at the catchment scale (i.e., watershed dynamics, see e.g., Georgakakos et al., 2004; Sikorska et al., 2012; Del Giudice et al., 2015; Azizian, 2018; Ravazzani et al., 2019; Tscheikner-Gratl et al., 2019; Wang et al., 2021; Radinja et al., 2021; Troin et al., 2022; Li et al., 2022; Saavedra et al., 2022) and/or to define the characteristic time behavior of a rainfall event (e.g., Courdent et al., 2017; Zhang et al., 2019; Tirpak et al., 2021; Lee et al., 2021; Saimy et al., 2022). New approaches to GSA have been recently developed to address model uncertainty within multi-model sensitivity analysis framework (Dai and Ye, 2015; Dai et al., 2017, 2022; Dell'Oca et al., 2020; Yang and Ye, 2022). Such a multi-model GSA enables one to jointly address uncertainty in process models as well as parametric uncertainty within each of these. Thus, understanding the joint impact of all of the aforementioned sources of uncertainty (i.e., related to

conceptual-mathematical model formulations and associated parametrization) on the functioning of a LID infiltration system is critical for a proper and long-term effective design.

Here, we focus on soakaways (or drainage wells, or similar infiltration devices), which are usually used in the context of small urban catchments (e.g., Riva et al., 2013; Roldin et al., 2013). We investigate how their design and the assessment of their functioning are affected by (*i*) multiple sources of uncertainty linked to the model (and related parameters) adopted to describe the rainfall event and the urban catchment, as well as by (*ii*) key characteristics of the subsurface system and of the structure itself. Our specific goal is to quantify the probability of failure of the soakaway system (see a sketch of the type of structure we consider in Fig. 1). The latter is defined as the probability that hydraulic head within the soakaway is larger than the structure height, thus yielding waterlogging and/or flooding. We do so by leveraging on the recent multi-model GSA developed by Dell'Oca et al. (2020). Starting from the observation that predictions based on a single model can result in statistical bias and overconfidence in the outcomes (e.g., Burnham and Anderson, 2002; Bredehoeft, 2005; Poeter and Anderson, 2005; Beven, 2006; Clark et al., 2008; Whling and Vrugt, 2008; Ye et al., 2008), these authors propose a set of indices to assess the sensitivity of the statistical moments of the probability density function of a performance metric of interest with respect to imperfect knowledge of (*a*) the model formulation employed to characterize the system behavior and (*b*) the ensuing parametrization. Here, we further and significantly extend the work of Dell'Oca et al. (2020) to embed a rigorous quantification of the sensitivity of the probability of failure (PF) of a system within a multi-model context. As an additional element of novelty, we also perform a process-based GSA to explore and quantify the relevance on PF of the various processes involved in our system. We then show how our approach can be employed through an exemplary application focused on a representative case associated with the preliminary design phase of an infiltration structure serving a region in the northern part of Italy.

The study is organized as follows. Sections 2 illustrates the modeling strategy in terms of the problem set-up (Section 2.1), the main theoretical elements associated with Global Sensitivity Analysis framed in a single- and a multi-model context (Section 2.2), and the target region together with the set of models considered (Section 2.3). Section 3 summarizes our key results in the context of a Single- and Multi-Model context and Section 4 provides our major conclusions.

2. Materials and methods

This Section is devoted to introducing the problem set-up (Section 2.1), including possible modeling choices we employ to depict (*i*) the rainfall event (Section 2.1.1) and watershed dynamics (Section 2.1.2) here considered as well as (*ii*) the interaction between the surface and the subsurface environment (Section 2.1.3). Section 2.2 describes the indices/metrics quantifying the sensitivity of the probability of failure of the structure with respect to (typically uncertain) model parameters within a single- and a multi-model context (Sections 2.2.1 and 2.2.2, respectively). Section 2.3 illustrates the study area, the collection of models considered and their uncertain parameters.

2.1. Problem set-up

2.1.1. Design rainfall event

A key step in the design of an infiltration structure is the definition of the design rainfall event (i.e., the design storm). Here, we employ the widely used power law formulation (e.g., Gupta and Waymire, 1990; Burlando and Rosso, 1996) of the depth-duration-frequency curve, DDF

$$h_{d,T_R} = h_{1,T_R} d^n; \qquad \text{with} \quad h_{1,T_R} = a_1 w_{T_R} \tag{1}$$

where h_{d,T_R} [L] is the rainfall depth associated with a rainfall event of assigned duration, d [T], and return period, T_R [T]; n [-] is a scale coefficient; a_1 [LT^{-n}] is the mean value of the maximum annual rainfall depth, $h_{\max}$, for a unit rain duration; and w_{T_R} [-] is the growing factor, corresponding to the value of the normalized random variable $W = h_{\max}/E[h_{\max}]$ associated with the non-exceedance probability $F(w = w_{T_R}) = (T_R - 1)/T_R$. Evaluation of w_{T_R} in Eq. (1) requires knowledge of the probability distribution of W. Here, we adopt the widely used generalized extreme value distribution, GEV (Coles, 2001; Yeo et al., 2021)

$$F(w) = e^{-t(w)}; \text{ with } t(w) = \begin{cases} \left(\Gamma(1+k) - k\dfrac{w-1}{\alpha}\right)^{1/k} & \text{if } k \neq 0 \\ e^{-\left(\frac{w-1}{\alpha}+\gamma\right)} & \text{if } k = 0 \end{cases} \tag{2}$$

where $\alpha > 0$ and $k > -1$ are the scale and shape parameters of the distribution, respectively, and $\gamma \approx 0.5772$ is the Euler's constant. Note that Eq. (2) reduces to the Gumbel distribution when $k = 0$. From Eq. (2) one obtains the values of w_{T_R} to be used in Eq. (1) as

$$w_{T_R} = \begin{cases} 1 + \dfrac{\alpha}{k}\left\{\Gamma(1+k) - \left(\ln\dfrac{T_R}{T_R-1}\right)^k\right\} & \text{if} \quad k \neq 0 \\ 1 - \alpha\left\{\ln\left(\ln\dfrac{T_R}{T_R-1}\right) + \gamma\right\} & \text{if} \quad k = 0 \end{cases}. \tag{3}$$

Synthetic hyetographs, describing the temporal variation of rainfall intensity consistent with values of h_{d,T_R} computed by Eq. (1), are typically adopted for the design of an infiltration structure. Here, we consider two widely used alternative models. These correspond to (*i*) the uniform, $i^U_{d,T_R}(t)$, and (*ii*) the Chicago, $i^C_{d,T_R}(t)$, hyetographs, respectively rendered by

$$i^U_{d,T_R}(t) = \frac{h_{d,T_R}}{d}; \quad \text{with} \quad 0 \le t \le d \tag{4}$$

$$i^C_{d,T_R}(t) = n\frac{h_{d,T_R}}{d}\begin{cases} \left(\dfrac{t_p - t}{t_p}\right)^{n-1} & \text{if } 0 \le t \le t_p \\ \left(\dfrac{t - t_p}{d - t_p}\right)^{n-1} & \text{if } t_p < t < d \end{cases} \tag{5}$$

While the uniform hyetograph is constant across the temporal window within which it is defined, the Chicago model considers an initial period of growth of the rain intensity until a peak value is attained (at time t_p [T]), which is then followed by a decrease of rain intensity. The peak time can be formulated as a fraction of the rain event duration, i.e., $t_p = rd$, with $0 < r < 1$ and usually ranging between 0.3 and 0.5 (e.g., Liao et al., 2021).

2.1.2. Rainfall-runoff model

The flowrate at the closure section of a given urban catchment, i.e., $Q_e(t)$ [L^3T^{-1}], can be evaluated through the following convolution integral

$$Q_e(t) = \varphi_m S \int_0^t i_{d,T_R}(t-\tau)u(\tau)d\tau \tag{6}$$

where S [L^2] is the area encompassed by the urban catchment, φ_m [-] is the runoff coefficient, and $u(\tau)$ [T^{-1}] is the instantaneous unit hydrograph (IUH), i.e., the catchment response to a pulse-like instantaneous rain event. We recall that $u(\tau)$ reflects the main hydrological characteristics of the watershed and several empirical models have been proposed in the literature to estimate it. A common approach that has been seen to be adequate in small catchments (e.g., Buytaert et al., 2004) is based on the linear reservoir model, which is expressed through

$$u(t) = e^{-t/\lambda}/\lambda \tag{7}$$

where λ [T] is the reservoir constant. Here, we set

$$\lambda = 0.65^{1/(1-n)} T_c \tag{8}$$

T_c [T] being the corrivation (or concentration) time, i.e., the time required for the furthest water particle to reach the drainage structure. Note that making use of Eq. (8) in the linear reservoir model yields the same maximum value of Q_e as the classical kinematic model when a uniform rain intensity is considered (details not shown). Several empirical (or semi-empirical) formulations have been proposed to evaluate T_c as a function of the basin features (e.g., Azizian, 2018; Ravazzani et al., 2019 and references therein). Here, consistent with the methodological focus of our study, we adopt the formulation of Ventura (1905), that is widely used for small catchment areas (<10 km^2)

$$T_c = 0.1272\sqrt{S/i} \tag{9}$$

where i [-] is the slope of the main drainage branch of the catchment, T_c is given in hours and S in km^2. If T_c is negligible (with respect to the duration of the rain and the drainage time linked to the infiltration structure), then $u(t) = \delta(t)$ and Eq. (6) reduces to

$$Q_e(t) = S\varphi_m i_{d,T_R}(t) \tag{10}$$

2.1.3. Infiltration structure

We focus on a scenario associated with a cylindrical drainage well of diameter D [L] (i.e., with bottom surface $A = \pi D^2/4$) and height H [L] (see Fig. 1 for a sketch of the structure). Water mass balance within the well drives the water level inside the structure, i.e., $h_w(t)$ [L], according to

$$A\frac{dh_w(t)}{dt} = Q_e(t) - Q_{inf}(t) \tag{11}$$

where Q_{inf} [L^{3}T^{-1}] is the outlet flowrate from the soakaway. The evaluation of Q_{inf} requires the solution of the three-dimensional partially saturated flow field (as rendered, e.g., through the Richards' formulation), describing the spatial and temporal evolution of the wetting front, as well as the knowledge of the properties of the underlying soil (such as unsaturated hydraulic conductivity and porosity). Empirical and semi-empirical formulations have been developed with the aim of circumventing the need for solving the highly non-linear Richards' problem. A widely used semi-empirical formulation has been proposed by Sieker (1984). According to the latter Q_{inf} is estimated as

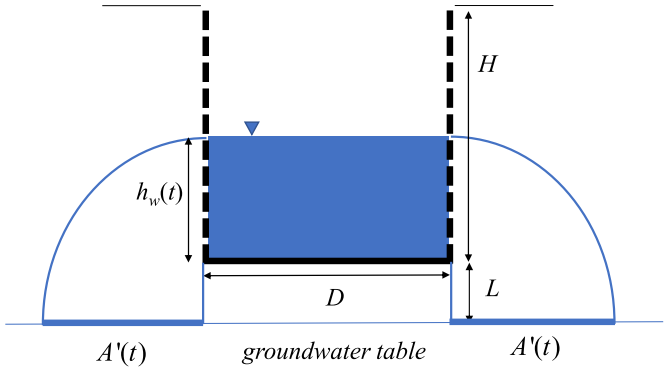

Fig. 1. (a) Sketch of the infiltration structure (drainage well) of diameter D and height H. The well bottom is at a distance L from the groundwater table. The water level inside the structure, $h_w(t)$, and the effective drainage area of the structure, $A'(t)$, are time dependent variables.

$$Q_{inf}(t) = A'(t)\frac{K_s}{2}\frac{L + h_w(t)}{L + 0.5h_w(t)};$$
$$\text{with } A'(t) = \frac{\pi}{4}\left[(D + h_w(t))^2 - D^2\right] \tag{12}$$

Here, $A'(t)$ [L^2] is the effective drainage area of the structure and L is the distance between the bottom of the well and the groundwater table (see Fig. 1). Note that Eq. (12) holds under the following assumptions: (*i*) the bottom of the infiltration structure is impervious, a situation that is often encountered after a prolonged period of operation due to clogging effects (e.g., Emerson et al., 2010), (*ii*) L is constant, i.e., L is not significantly affected by the drainage, (*iii*) the unsaturated conductivity is set equal to $K_s/2$, K_s being the saturated hydraulic conductivity of the soil (e.g., Bouwer, 1969), (*iv*) the vertical hydraulic gradient is approximated by considering a characteristic length of $(L + h_w/2)$, and (*v*) the flow leaving the well through the lateral surface is conceptualized via a parabolic model, so that the radius of the mean lateral distance of the wetting front from the structure can be approximated as $h_w/2$.

2.2. Global Sensitivity Analysis

2.2.1. Single-model sensitivity analysis

Following Dell'Oca et al. (2017) and La Cecilia et al. (2020), the sensitivity of the probability of failure (PF) of a system described by a single- (conceptual/mathematical) model with respect to the i-th uncertain model parameter (x_i) is quantified through the quantity

$$AMAP_{x_i} = \int_{\Gamma_{xi}} \left|1 - \frac{P_{F|x_i}}{P_F}\right| \rho_{x_i} dx_i \tag{13}$$

where P_F is the unconditional probability of system failure (SF) and $P_{F|x_i}$ is its counterpart conditional to a given value of parameter x_i, ρ_{x_i} being the probability density function (pdf) of x_i defined across the support Γ_{x_i}. In this framework, index $AMAP_{x_i}$ quantifies sensitivity in terms of the variation of PF induced by the variability of parameter x_i of the selected model.

2.2.2. Multi-model sensitivity analysis

Here, we ground our study on the work of Dell'Oca et al. (2020) and extend the metric given by Eq. (13) to encompass a multi-model context. We do so upon introducing an original index, termed $AMAP_{x_i^{M_j}}$, quantifying the effect of the i-th uncertain parameter (i.e., $x_i^{M_j}$) of model M_j (comprised in a set of N candidate interpretive models) on the probability of system failure. Such a metric is defined as

$$AMAP_{x_i^{M_j}} = \underbrace{w_{M_j}\frac{\left|P_F^{\boldsymbol{M}} - P_F^{M_j}\right|}{P_F^{\boldsymbol{M}}}}_{between-models} + \underbrace{w_{M_j}\int_{\Gamma_{x_i^{M_j}}} \frac{\left|P_F^{M_j} - P_{F|x_i^{M_j}}\right|}{P_F^{\boldsymbol{M}}} \rho_{x_i^{M_j}} dx_i^{M_j}}_{within-model};$$
$$\text{with } P_F^{\boldsymbol{M}} = \sum_{j=1,N} w_{M_j} P_F^{M_j} \tag{14}$$

where, $P_F^{\boldsymbol{M}}$ is the unconditional PF evaluated within a multi-model context, i.e., upon considering the whole set of N available models and their uncertain parameters; $P_F^{M_j}$ is the value of PF conditional to model M_j; $P_{F|x_i^{M_j}}$ is the value of PF conditional to parameter $x_i^{M_j}$ and model M_j; w_{M_j} is the weight related to model M_j (see, e.g., Neuman, 2003; Ye et al., 2004; Poeter and Hill, 2007; Höge et al., 2019); and $\rho_{x_i^{M_j}}$ is the (marginal) pdf of parameter $x_i^{M_j}$ defined across the support $\Gamma_{x_i^{M_j}}$. Note that index $AMAP_{x_i^{M_j}}$ quantifies the sensitivity of PF to the uncertain parameter $x_i^{M_j}$ as the sum of (*i*) a *between-models*, and (*ii*) a *within-model*

contribution. The former is associated with uncertainty in the model formulation. The latter provides an appraisal of the variability of PF due to the variability of parameter $x_i^{M_j}$ when model M_j has been selected. Note also that the between-models component in Eq. (14) vanishes and Eq. (14) reduces to Eq. (13) when only one model is included in the analysis.

Relying on the index $AMAP_{x_i^{M_j}}$ enables one to address questions such as 'How does the probability of failure of a system of interest changes if we fix the value of an otherwise uncertain parameter (i.e., $x_i^{M_j}$) appearing in model M_j?' In this context, it is worth noting that even as diverse models of the collection might be associated with parameters with the same conceptual-physical meaning, we treat them as distinct quantities.

According to Eq. (13) and Eq. (14), the single- and multi-model sensitivity indices are linked through

$$AMAP_{x_i^{M_j}} = \underbrace{\frac{w_{M_j}}{P_F^{\boldsymbol{M}}}\left|P_F^{\boldsymbol{M}} - P_F^{M_j}\right|}_{between-models} + \underbrace{\frac{w_{M_j}}{P_F^{\boldsymbol{M}}}P_F^{M_j}AMAP_{x_i}}_{within-model} \tag{15}$$

Therefore, while (in general) $AMAP_{x_i^{M_j}} \neq AMAP_{x_i}$, the multi-model index can be larger or smaller than its single model counterpart, depending on the model weight and on the ratio $P_F^{M_j}/P_F^{\boldsymbol{M}}$, while the following inequalities are always satisfied

$$w_{M_j}\frac{P_F^{M_j}}{P_F^{\boldsymbol{M}}}AMAP_{x_i} < AMAP_{x_i^{M_j}} < \frac{w_{M_j}}{P_F^{\boldsymbol{M}}}\left(1 + P_F^{M_j}AMAP_{x_i}\right) \tag{16}$$

This aspect will be further elucidated in Section 3.

2.3. Study area: uncertain models and parametrization

Solution of Eq.s (1)–(12) requires specifying the values of a set of parameters associated with a given model employed to depict the system. Here we tie our analysis to the context of the preliminary design phase of an infiltration structure of the kind that is planned for future developments of urban areas in the region around the city of Lecco (Fig. 2), located in the Lombardia Region (northern Italy). In this framework, we analyze a synthetic catchment whose characteristics are representative of the target urban area. Doing so enables us to explore jointly the influence of main (uncertain) characteristics of (*a*) the rain event, (*b*) the catchment, and (*c*) the subsurface environment on the PF of the target structure. Table 1 lists the set of parameters pertaining to the characterization of the rain event, the dynamics of the urban catchment and the functioning of the infiltration structure. We consider a mixture of (*i*) deterministically known and (*ii*) uncertain model parameters. While the former correspond to parameters that are typically considered as readily inferable from commonly available data, the latter are chiefly related to intrinsic environmental variability. Values of deterministic quantities listed in Table 1 are related to the description of the rain event and are set to those that have been established and are typically used for the Province of Lecco (datasets included in the open-access portal: www.idro.arpalombardia.it). Uncertain parameters (highlighted with a grey background in Table 1) encompass both surface and subsurface hydrology aspects typical of the area considered. Finally, we also explore the impact of the structure design variables (D and H, highlighted in yellow in Table 1) on PF. In this context, each uncertain parameter and design variable is treated as an independent random quantity, associated with a uniform pdf, i.e., $\rho_{x_i} = [\max(x_i) - \min(x_i)]^{-1}$ ($\max(x_i)$ and $\min(x_i)$ correspond to the upper and lower bound of the range of variability of parameter x_i, respectively, and are included in Table 1). The choice of a uniform pdf enables one to assign equal weight to all values of a distribution, a scenario which is common in the absence of prior information. Note that we employ the same parameter densities in the multi-model context, i.e., $\rho_{x_i^{M_j}} = \rho_{x_i}$. We note that the ranges of values adopted to characterize the rain event as well as the surface and subsurface system are also typical of urban environments of the kind we consider and are associated with coefficients of variation of the order of 50%. The large variability assigned to the return period (from 10 to 100 years) has been selected on the basis of literature results and is consistent with the observed increase in the frequency of extreme events and/or the increase rainfall intensity for fixed T_R (see Section 1). Finally, design variables are allowed to vary across values typically encountered in practical applications, consistent with the design phase we consider (e.g., Woods-Ballard et al., 2007).

Regarding the set of models of interest, we analyze combinations stemming from (*a*) two formulations of the IDF curves, (i.e., the Uniform and the Chicago hyetographs) and (*b*) two formats of the IUH (i.e., the linear reservoir model and its counterpart corresponding to a time of response of the reservoir which is virtually zero). Therefore, our multi-model analysis encompasses a collection of four models.

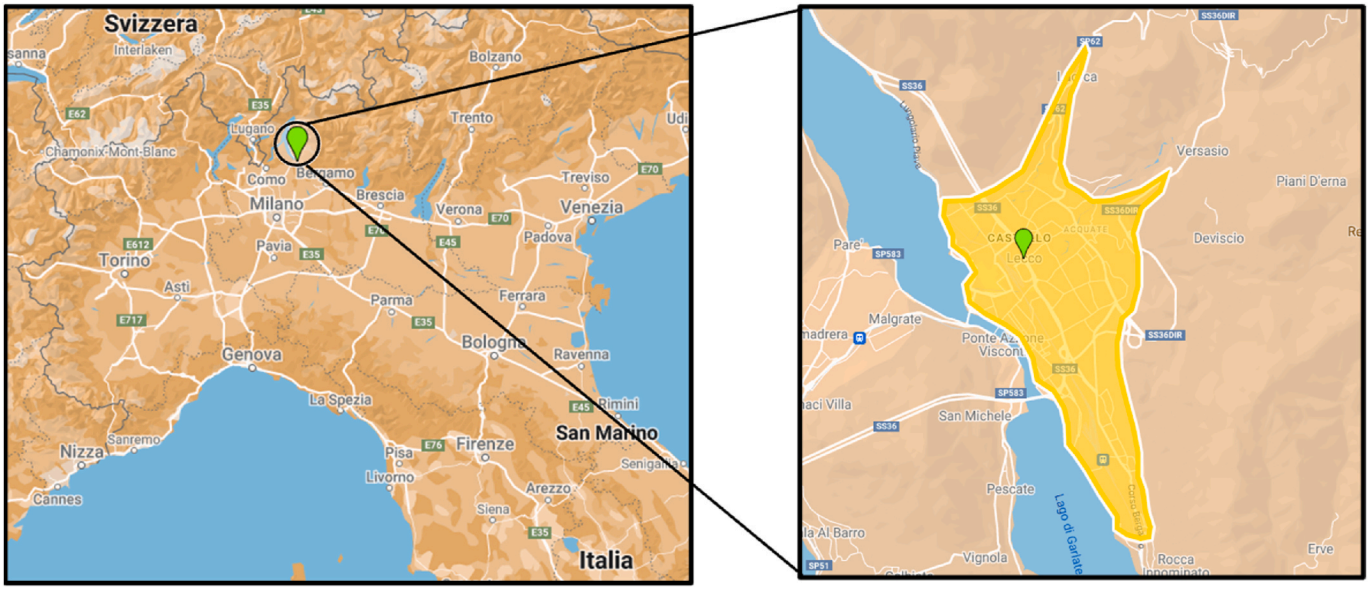

Fig. 2. Geographical location of the urban area of reference for the study, corresponding to the surroundings of the city of Lecco (Lombardia Region, northern Italy).

Table 1
List of model parameters, including values of the deterministically fixed parameters and intervals of variability of the uncertain model parameters (shadowed background) considered in the study. Design variables are highlighted in yellow. Values of quantities related to the description of the rain event correspond to those that are typically used for the Province of Lecco (northern Italy; see datasets included in the open-access portal: www.idro.arpalombardia.it). Values of model parameters correspond to surface and subsurface hydrology aspects typical of the area considered.

	Description	Parameter	Value	Unit
Rain Event	Scale coefficient	n	0.5	-
	Mean of the maximum rain depth with $d = 1$	a_1	29.42	$mm\ hr^{-n}$
	Shape parameter of the GEV distribution	k	-0.246	-
	Scale parameter of the GEV distribution	α	0.31	-
	Peak time/d	r	0.4	-
	Duration of the rainfall event	d	$0.1 - 24$	hr
	Return period	T_R	$10 - 100$	yr
Urban Catchment, UC	Runoff coefficient	φ_m	$0.3 - 0.9$	-
	Area encompassed by the UC	S	$0.001 - 0.01$	km^2
	Slope of the main branch of the UC	i	$0.001 - 0.5$	-
Subsurface environment	Distance: bottom of soakaway and water table	L	$0.01 - 5$	m
	Saturated hydraulic conductivity	K_s	$10^{-6} - 10^{-1}$	$m\ s^{-1}$
Infiltration Structure	Diameter of the structure	D	$0.5 - 2$	m
	Height of the structure	H	$1 - 2$	m

- Model Set *UL*: uniform hyetograph Eq. (4) and linear reservoir model Eq.s (6)–(9);
- Model Set *UI*: uniform hyetograph Eq. (4) and reservoir characterized by a negligible corrivation time Eq. (10);
- Model Set *CL*: Chicago hyetograph Eq. (5) and linear reservoir model Eq.s (6)–(9);
- Model Set *CI*: Chicago hyetograph Eq. (5) and reservoir characterized by a negligible corrivation time Eq. (10).

Model sets *CL* and *UL* share the same vector of uncertain model parameters and design variables, i.e., $\boldsymbol{x}^{UL} = \boldsymbol{x}^{CL} = [T_R; d; \varphi_m; S; i; D; H; L; K_s]^{\mathrm{T}}$. Note that, since the corrivation time is negligible in *UI* and *CI*, neither of these models includes the parameter i (required for the evaluation of the corrivation time, see Eq. (9)), i.e., $\boldsymbol{x}^{UI} = \boldsymbol{x}^{CI} = [T_R; d; \varphi_m; S; D; H; L; K_s]^{\mathrm{T}}$.

We solve Eq.s (6)–(12) numerically through a finite difference scheme. Uncertainty (or variability) about model parameters and design variables propagates onto the target performance metric, i.e., the water level in the infiltration structure ($h_w(t)$), that can be treated as a random quantity. We consider the soakaway to be appropriately designed if, as a consequence of a rain event, $h_w(t)$ is always (i.e., at all times) smaller than the well height, H. Otherwise, failure of the hydraulic structure takes place when the water level reaches (at least once during operation) the height of the well. To quantify system failure (SF) we introduce a random indicator I defined as

$$I = \begin{cases} 0 & if \quad \forall t \quad h_w(t) < H \\ 1 & if \quad \exists t | \quad h_w(t) = H \end{cases} \tag{17}$$

Therefore, SF is detected when $I = 1$ and the unconditional PF within a single model context, P_F, coincides with the probability of I being equal to one, i.e., $P_F = P(I = 1)$. For completeness, Table 2 lists the most relevant acronyms and symbols employed in the study.

Table 2
Summary of acronyms and relevant symbols.

Acronym/ Parameter	Description
LID	Low impact development
SA	Sensitivity Analysis
LSA	Local Sensitivity Analysis
GSA	Global Sensitivity Analysis
IDF	Intensity-duration-frequency
DDF	Depth-duration-frequency
IUH	Instantaneous unit hydrograph
UL	Uniform hyetograph and linear reservoir model
UI	Uniform hyetograph and reservoir characterized by a negligible corrivation time
CL	Chicago hyetograph and linear reservoir model
CI	Chicago hyetograph and reservoir characterized by a negligible corrivation time
PF	Probability of system failure
SF	System failure
P_F	Unconditional Probability of SF; single model context
$P_{F\|x_i}$	Probability of SF conditional to a given value of parameter x_i; single model context
$P_F^{\boldsymbol{M}}$	Unconditional probability of SF; multi-model context
$P_F^{M_j}$	Probability of SF conditional to model M_j; multi-model context.
$P_{F\|x_i^{M_j}}$	Probability of SF conditional to parameter $x_i^{M_j}$ and model M_j; multi-model context
$P_{F\|x_i^{(k,M_j)}}$	Probability of SF conditional to parameter x_i of process P^k and model M_j; multi-model context
$AMAP_{x_i}$	Sensitivity index for the probability of system failure w.r.t. parameter x_i; single model context
$AMAP_{x_i^{M_j}}$	Sensitivity index for the probability of system failure w.r.t. parameter $x_i^{M_j}$ of model M_j; multi-model context
$AMAP_{P^k}$	Sensitivity index for the probability of failure w.r.t. the k-th system process; multi-model context

3. Results

In the following we illustrate the key results obtained with a single- and a multi-model approach. For each candidate model (i.e., for each of the four models considered in Section 2.3) we randomly sample each uncertain parameter and design variable from its associated uniform distribution (defined across the support listed in Table 1). We then solve

Eq.s (6)–(12) for the obtained (Monte Carlo, MC) parameter realizations. Note that, for a given parameter set, we stop our computation (*i*) when SF is detected (i.e., if $I = 1$) or (*ii*) at a time equal to $10 \times \max\{d, \lambda\}$ if no SF is detected (i.e., $I = 0$).

When considering a single-model approach, we evaluate the (unconditional) probability of system failure, P_F, associated with the use of each model on the basis of a set of 10^6 MC simulations. The probability of system failure conditional to a value of parameter x_i (i.e., $P_{F|x_i}$ in Eq. (13)) is evaluated by (*i*) setting parameter x_i to a given value (we employ 60 equally sized bins to discretize the support of each parameter); and then (*ii*) performing 10^5 MC realizations through random sampling of the remaining model parameters.

Within a multi-model approach, we consider all models in the set to be characterized by equal weights (or model probability), i.e., $w_{UL} = w_{UI} = w_{CL} = w_{CI} = 0.25$. This choice reflects the observation that all models are equally likely a priori. We then compute the unconditional PF (denoted as $P_F^{\boldsymbol{M}}$) by making use of Eq. (14) and on the basis of 10^6 MC simulations performed for each candidate model (for a total of 4×10^6 MC simulations). We finally evaluate the conditional PF (denoted as $P_{F|x_i^{M_j}}$) by repeating steps (*i*)-(*ii*) described above for each model.

3.1. Single-model sensitivity analysis

This Section focuses on the sensitivity of the probability of failure of the infiltration structure with respect to the uncertain model parameters within a single-model context. We recall that this is tantamount to conditioning the results on the choice of a given interpretive conceptual/mathematical model.

We start by briefly analyzing the general behavior of the system considering each of the models detailed in Section 2.3. Fig. 3 depicts the temporal evolution of (*a*) Q_e (continuous curves), Q_{inf} (symbols), and (*b*) h_w (the structure height, H, is also depicted as reference; see the horizontal dashed line) considering an exemplary combination of randomly sampled model parameters. We note that employing a Chicago hyetograph imprints a strong and sudden increase to the values associated with the temporal history of Q_e, leading to failure of the drainage structure. The peak value is less pronounced for the *CL* than for the *CI* model set (see inset in Fig. 3a). Otherwise, SF is not observed when the Uniform hyetograph is adopted for the combination of model parameters selected for this illustrative example. In this case, Q_e stabilizes at a constant value that is not significantly impacted by the selected type of IUH. Moreover, since $Q_e \approx Q_{inf}$ a constant value of $h_w < H$ is attained.

We then investigate the impact of the various uncertain model parameters and design variables listed in Table 1 on PF by inspecting the results depicted in Fig. 4. The latter depicts the conditional PF, $P_{F|x_i}$, as a function of each model parameter x_i (intervals of variability of each parameter are rescaled within the unit range for ease of interpretation) for the (a) *UL*, (b) *UI*, (c) *CL*, and (d) *CI* model sets. The unconditional single-model PF (P_F; horizontal black continuous lines) is also depicted as reference together with its unconditional multi-model counterpart ($P_F^{\boldsymbol{M}}$; horizontal dashed grey line). A detailed analysis of the latter is

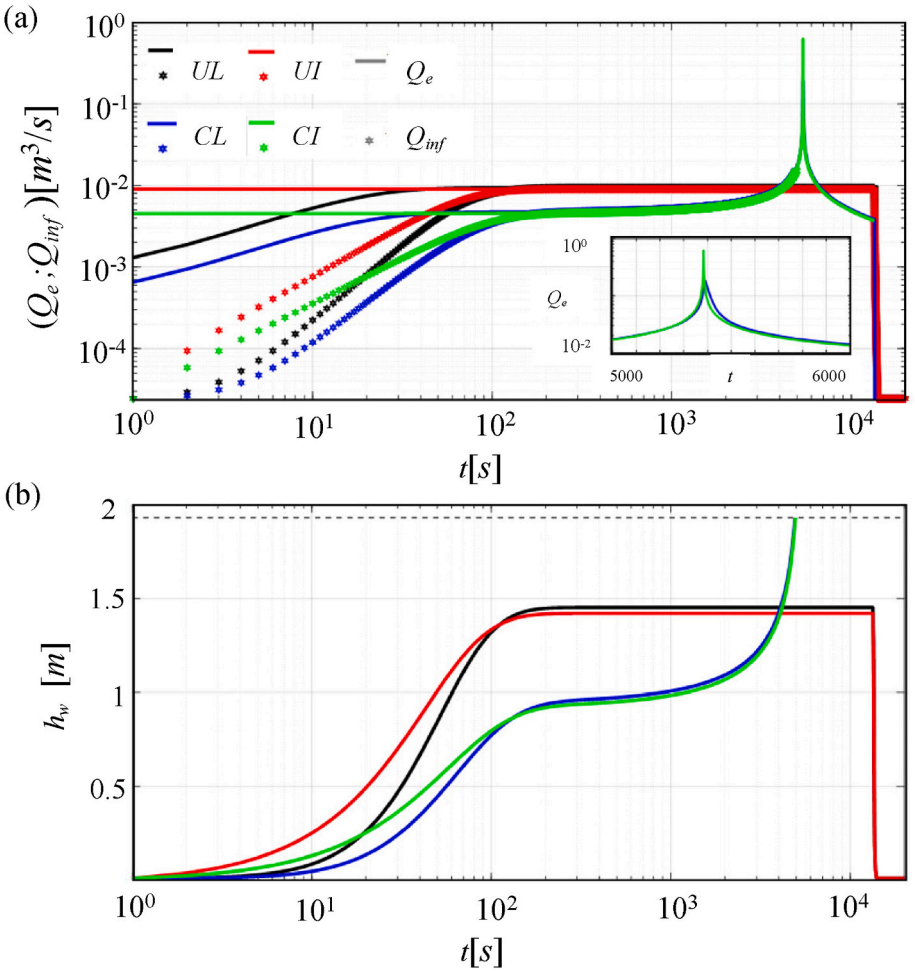

Fig. 3. (a) Flowrate at the closure section of the urban catchment, i.e., $Q_e(t)$ (continuous curves), and outlet flowrate from the infiltration structure, i.e., $Q_{inf}(t)$ (symbols). (*b*) Water level inside the structure, i.e., $h_w(t)$ (continuous curves), and the structure height, i.e., H (horizontal dashed line). Results are for an examplary combination of random parameters. The inset highlights the peak value of $Q_e(t)$ for the *CL* and *CI* models.

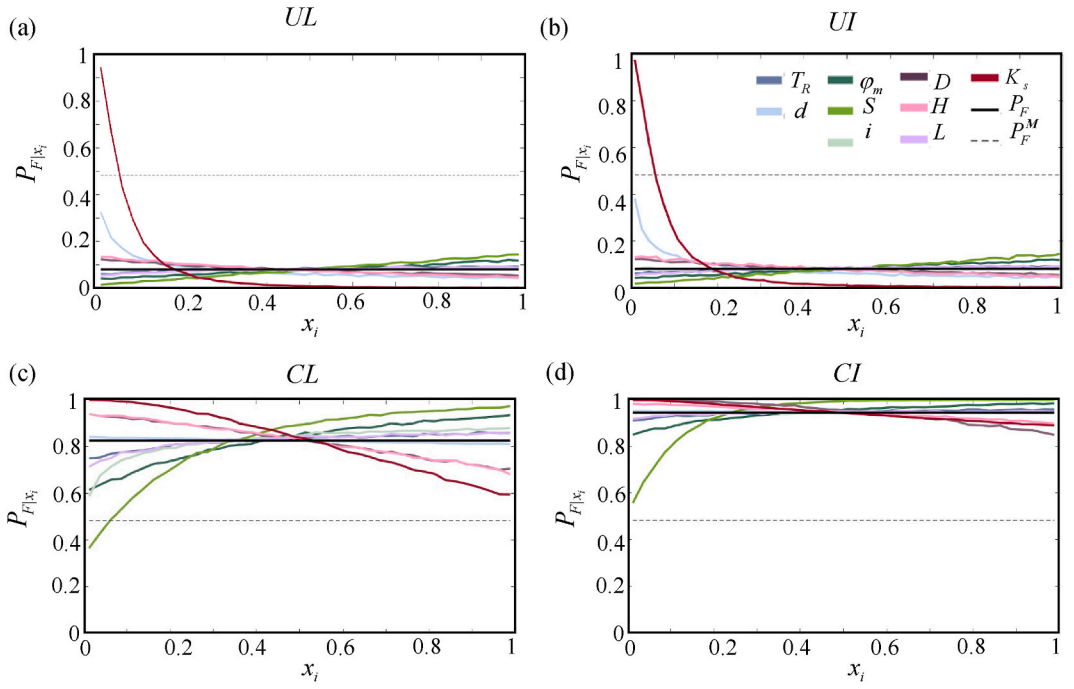

Fig. 4. Unconditional probability of failure, i.e., P_F (horizontal black lines) and conditional probability of failure, i.e.,$P_{F|xi}$. Intervals of variability of each parameter are rescaled between 0 and 1 for ease of interpretation. Results are for (a) *UL*, (*b*) *UI*, (*c*) *CL* and (*d*) *CI* model sets. The unconditional multi-model probability of failure, i.e., $P_F^{\boldsymbol{M}}$ (horizontal dashed grey line) is also depicted.

offered in Section 3.2.

Inspection of Fig. 4 reveals that adopting the Chicago hyetograph (see Fig. 4c–d) leads to (overall) higher values of PF than their counterparts associated with the Uniform hyetograph (see Fig. 4a–b). This finding is consistent with the behaviors detected and discussed in Fig. 3. Selecting the Uniform hyetograph and varying the format of the IUH (compare Fig. 4a and b) does not lead to noticeable discrepancies in the values of P_F or $P_{F|x_i}$. This result is related to the tendency of reaching very similar late-time values of h_w for the *UI* and *UL* model sets (as also noted in Fig. 3 and further discussed in the following). Considering the Chicago hyetograph, the *CL* model set leads to smaller value of P_F than its counterpart stemming from the *CI* model set. This result is in line with the reduced peak value of Q_e observed in Fig. 3 for *CL* with respect to *CI*. We further note that employing the *CL* model set yields an increased variability of $P_{F|x_i}$ due to parameter uncertainty and variability of design variables. The latter finding is consistent with the observation that the temporal behavior associated with (*i*) the rain intensity for the Chicago hyetograph and (*ii*) the catchment response for the Linear IUH tends to enhance the degree of variability of Q_e and Q_{inf} in response to variations of model parameter values.

Analysis of Fig. 4a-b reveals that when considering the Uniform hyetograph (regardless of the adopted IUH, i.e. for UL, UI) PF is strongly influenced by the hydraulic conductivity of the soil surrounding the drainage well (i.e., K_s). Values of PF are particularly high (and close to 1) if the subsurface is characterized by a low-permeable medium and tend to vanish for large K_s values. These results suggest that the efficiency of an infiltration structure would primarily benefit from a detailed analysis and characterization of the subsurface system. Moreover, PF tends to increase for events characterized by a short duration (i.e., small values of *d*). Such a scenario corresponds to a strong rain intensity that promotes failure of the structure. An increase in the drainage coefficient (i.e., φ_m) and in the catchment area (i.e., *S*) yields a correspondingly similar (albeit only slight) increase of PF. The documented similarity of the trends of $P_{F|S}$ and $P_{F|\varphi_m}$ is linked to the format of the convolution integral (see Eq. (6)). It also suggests that the impact of the uncertainty of *S* as a parameter involved in the definition of the corrivation time (see Eq. (9)) is not relevant for the test cases here analyzed. Variations of the remaining model parameters (i.e., T_R, *i*, and *L* for *UL*; and T_R and *L* for *UI*) and design variables (*D* and *H*) do not induce significant variations in the probability of failure of the drainage structure. This, in turn, implies that the imperfect knowledge of climate conditions (as quantify by T_R) and the location of the groundwater water table (i.e., *L*) as well as the design variables (selected within intervals usually adopted in practical applications) are not too significant in the assessment of the probability of failure of the structure under the action of a Uniform hyetograph.

Otherwise, when considering the Chicago hyetograph, inspection of Fig. 4c-d reveals the following key features: (*i*) variations in K_s, φ_m, and *S* lead to strong variations in the conditional PF, independent of the IUH formulation considered (i.e. for CL, CI); (*ii*) $P_{F|i}$ increases with *i* for the *CL* model set since increasing *i* would lead to a faster catchment response, thus favoring higher values of Q_e and a higher PF; (*iii*) the design parameters of the drainage structure impact PF in a similar way (since both quantities are linked to the well storage volume). Similar to what observed for the Uniform hyetograph, PF is not significantly influenced by *L* and T_R also in the presence of a Chicago model. Moreover, consistent with the rainfall model adopted, also the rain duration does not induce marked variations in the values of PF. These results suggest that, with reference to the surface hydrology compartment of the system considered, the key role is played by the dynamics of the interaction between the catchment response (as rendered through the IUH) and the temporal evolution of the rain intensity (as rendered by the employed hyetograph).

Fig. 5a provides a synthesis of the results of the analysis by depicting the values of the single-model sensitivity indices $AMAP_{x_i}$ in Eq. (13) associated with the uncertain parameters and design variables for all models investigated. These results suggest that the adoption of the Uniform hyetograph leads to an overall larger degree of sensitivity to all parameters affected by uncertainty as compared to what can be observed when the Chicago hyetograph is employed. This behavior is due to the definition of the sensitivity index $AMAP_{x_i}$, where P_F (whose values are lower for *UL* and *UI* than their counterparts associated with *CL* and *CI*) appears at the denominator. When considering the *UL* or the

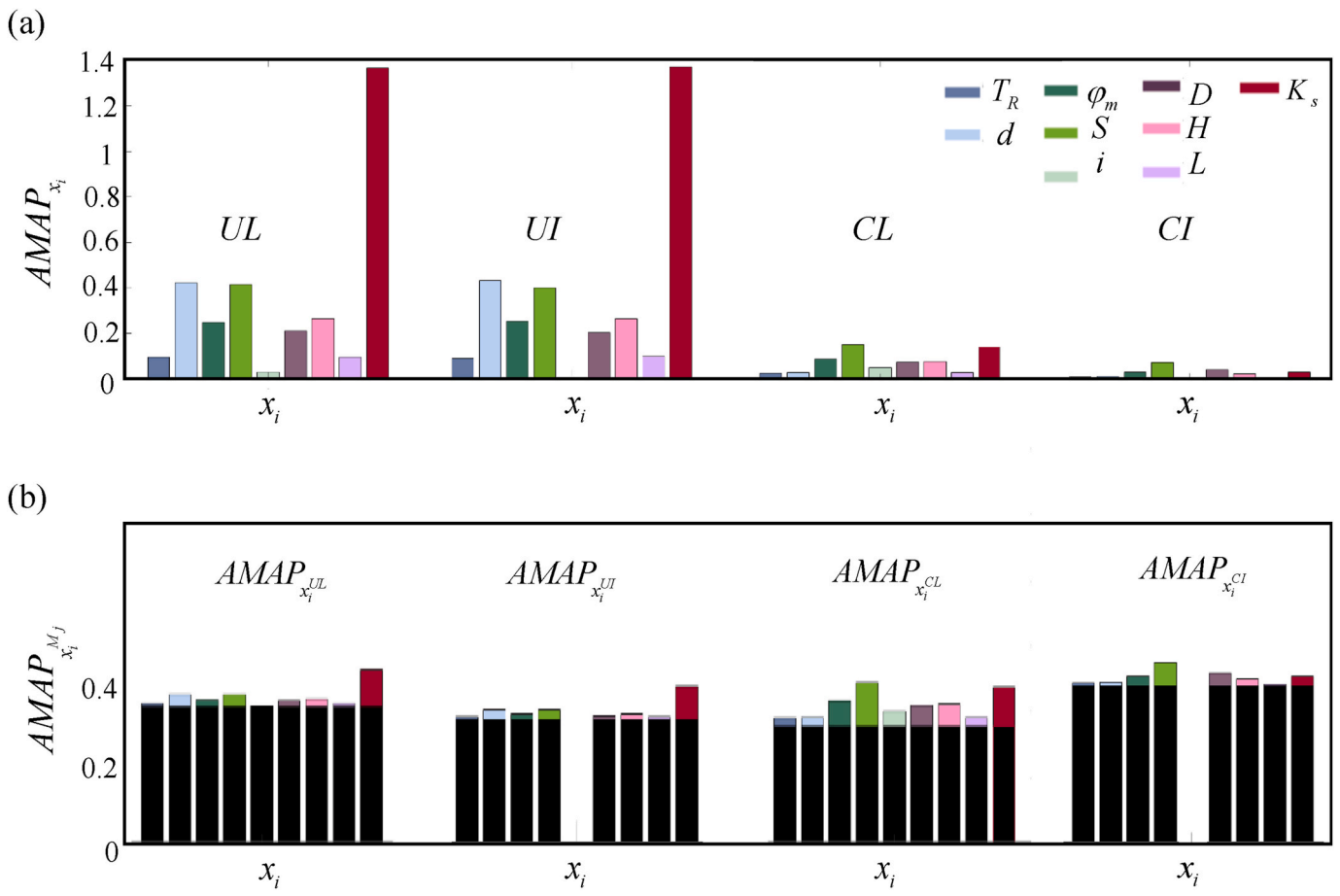

Fig. 5. (a) Single-model, $AMAP_{x_i}$ and (b) multi-models, $AMAP_{x_i}^{M_j}$, sensitivity indices for parameter x_i (see color legend) and models M_j = (*UL*; *UI*; *CL*; *CI*). The between-models contribution to $AMAP_{x_i}^{M_j}$ is highlighted in black. (For interpretation of the references to color in this figure legend, the reader is referred to the Web version of this article.)

UI model set, the dominant parameter is associated with the conductivity of the groundwater system, as quantified by the values of $AMAP_{K_s}$. In particular, one can note that $AMAP_{K_s} > 1$ because $P_{F|K_s} \gg P_F$ when the conductivity of the subsurface system is very low. Otherwise, the *CL* and *CI* model sets are characterized by a more even level of sensitivity to the influential parameters pertaining to the surface (i.e., S, φ_m, and eventually i for *CL*) and subsurface (K_s) compartments of the system as well as to the design variables (i.e., D and H).

3.2. Multi-model sensitivity analysis

In this Section we focus on the sensitivity of PF considering the collection of the four models analyzed, i.e., embedding model uncertainty in the analysis. The unconditional multi-model probability of failure P_F^M is depicted in Fig. 3a-d (horizontal dashed grey lines). Fig. 5b depicts the multi-model sensitivity indices, $AMAP_{x_i}^{M_j}$, associated with models M_j = *UL*, *UI*, *CL*, and *CI*.

As shown in Eq. (14), the between-models contributions of $AMAP_{x_i}^{M_j}$ (highlighted in black in Fig. 5b) represent the portion of the parameter sensitivity (in a multi-model context) that can be related to the discrepancy between the unconditional multi-model PF and its (unconditional) counterpart associated with a specific model considered. In the setting analyzed, we obtain very similar values for the between-models contributions to $AMAP_{x_i^{UL}}$ and $AMAP_{x_i^{UI}}$. This result is due to (*a*) the equal model weights (i.e., $w_{UL} = w_{UI} = 0.25$) considered and (*b*) the observation that the single model PF computed for *UL* (P_F^{UL}) and *UI* (P_F^{UI}) are almost identical, as shown in Fig. 4a-b. Otherwise, slightly smaller and larger values are observed for the between-models contributions related to $AMAP_{x_i^{CL}}$ and $AMAP_{x_i^{CI}}$, respectively (see Fig. 5b). This result is linked to the observation that $|P_F^M - P_F^{CL}| < |P_F^M - P_F^{UI}| < |P_F^M - P_F^{CI}|$ (see Fig. 4). Furthermore, we observe that the between-models contribution is key to each $AMAP_{x_i}^{M_j}$, reflecting the different values of $P_F^{M_j}$ associated with each of the distinct models considered. In other words, taking into account uncertainty in the model is critical to fully characterize the impact of parameters and design variables on PF.

Comparing single- and multi-model sensitivity indices reveals an overall agreement between the relative degree of sensitivity of PF to the various model parameters. One can note that K_s is the parameter showing the highest sensitivity in both the single- and multi-model contexts considering the Uniform hyetograph. At the same time, we note that the values of $AMAP_{x_i}^{M_j}$ are more evenly distributed amongst the various parameters than considering the corresponding results obtained within a single-model analysis. The latter behavior is consistent with the observation that in the multi-model context parameters that do not induce strong *within-model* contributions to PF, i.e., parameters with low values of $AMAP_{x_i}$, are still associated with non-negligible between-models contribution (related to the choice of the model where these appear). We further note that, considering *UL* and *UI*, we obtain $AMAP_{x_i}^{M_j} < AMAP_{x_i}$ (see Fig. 5), in agreement with the observation that $P_F^{UI} \approx P_F^{UL} \ll P_F^M$ (see Fig. 4) and Eq. (16). The opposite is documented

considering *CL* and *CI*, where $AMAP_{x_i^{M_j}} > AMAP_{x_i}$ (and $P_F^{CI} > P_F^{CL} \gg P_F^{M}$).

3.3. Impact of process uncertainty

We leverage on the results presented in Section 3.2 to provide an overall quantification of the impact of the uncertainty associated with each process (i.e., rain, runoff, and infiltration) on PF. We do so by re-casting Eq. (15) within a process-oriented framework (Dell'Oca et al., 2020). We then evaluate the sensitivity of PF with respect to the *k*-th system process, P^k, as

$$AMAP_{P^k} = \underbrace{\sum_{j=1}^{N_M^k} w_{M_j} \frac{\left| P_F^{M} - P_F^{M_j} \right|}{P_F^{M}}}_{between-models} + \underbrace{\sum_{j=1}^{N_M^k} w_{M_j} \sum_{i=1}^{N_p^{(k,M_j)}} \int_{\Gamma_{x_i^{(k,M_j)}}} \frac{\left| P_F^{M_j} - P_{F\left|x_i^{(k,M_j)}\right.} \right|}{P_F^{M}} \rho_{x_i^{(k,M_j)}} dx_i^{(k,M_j)}}_{within-model} \tag{18}$$

where N_M^k is the number of models within which process P^k appears; $x_i^{(k,M_j)}$ is the *i*-th parameter associated with the *k*-th process as described in model M_j; $P_{F\left|x_i^{(k,M_j)}\right.}$ is the value of PF conditional to parameter $x_i^{(k,M_j)}$; $N_p^{(k,M_j)}$ is the number of parameters $x_i^{(k,M_j)}$ associated with the *k*-th process as described in model M_j; and $\rho_{x_i^{(k,M_j)}}$ is the (marginal) pdf of $x_i^{(k,M_j)}$ defined across the support $\Gamma_{x_i^{(k,M_j)}}$. The sensitivity index $AMAP_{P^k}$ quantifies the degree of variability in PF (*i*) ascribable to the variability of P^k across the set of models within which P^k is implemented (*between-models* contribution) and (*ii*) due to the variability of PF with respect to the parameters pertaining to P^k (*within-model* contribution). In our case, $N_M^k = 4$ (with k = *rain*, *run* (for the runoff process), and *inf* (for the infiltration process)) for all of the three identified processes (i.e., all processes appear in all of the analyzed models). The number of parameters associated with each process across the ensemble of selected models is $N_p^{(rain,M_j)} = 2$ (i.e., T_R and *d*) and $N_p^{(inf,M_j)} = 4$ (i.e., K_S, *L*, *H*, and *D*) for all models considered (i.e., M_j = *UI*, *CI*, *UL*, and *CL*) while $N_p^{(run,M_j)} = 2$ (i.e., φ_m and *S*) for M_j = [*UI*; *CI*] and $N_p^{(run,M_j)} = 3$ (i.e., φ_m, *S*, and *i*) for M_j = [*UL*; *CL*].

Fig. 6 depicts $AMAP_{P^k}$ highlighting the *between-models* and *within-model* terms embedded in Eq. (18) as well as their relative contributions stemming from the diverse models here considered. All three processes are characterized by the same *between-models* contributions since all of them appear within each of the four models considered. The diverse components of the *between-models* contributions appear to be associated with identical strengths. This prevents one from neglecting any of the modeling formulations. Values of $AMAP_{inf}$ are the largest ones (due to a higher *within-model* contribution), followed by the $AMAP_{run}$ index. The smallest value is obtained for $AMAP_{rain}$, since the overall impact of T_R and *d* on PF is not critical for the test scenario considered.

4. Conclusions

We perform a rigorous (multi-model) Global Sensitivity Analysis (GSA) to assist the preliminary design phase of an infiltration (or drainage) structure (LID) in the context of an urban catchment. Doing so enables us to assess the relative impact of (*a*) model formulation and ensuing parametrization and (*b*) main design variables on the probability of failure (PF) of a LID. Regarding the (conceptual/mathematical) modeling approach employed to describe the system, we focus on the hydro-geological aspects (i.e., rain intensity, runoff and soil drainage capacity) as major source of uncertainty. We consider uniform (*U*) and Chicago (*C*) hyetographs combined with linear (*L*) and/or negligible corrivation time (*I*) reservoir models. This yields a collection of four distinct models (here termed *UL*, *CL*, *UI*, and *CI*) that reflects lack of deterministic knowledge about the system conceptualization. We perform the GSA within a single-model (i.e., each alternative model within the ensemble is consider as the reference one) and a multi-model (i.e., all of the alternative models in the ensemble are considered at the same time) framework to enable discriminating the contribution of the various sources of uncertainty considered to the variability of PF. In the multi-model context, we also perform a process-based GSA to quantify the relevance on PF of the various processes involved in our system.

Our results suggest that the adoption of the Uniform hyetograph leads to (overall) low values of PF and very similar behaviors for *UL* and *UI*. This suggests that the modeling choice about the reservoir model is not critical when the rain intensity is (approximately) uniform. The degree of variability of PF across the *UL* and *UI* model sets is dominated by the uncertainty associated with the hydraulic conductivity of the subsurface domain. Otherwise, considering a Chicago hyetograph yields (overall) higher values of PF while, at the same time, PF is less sensitive with respect to the diverse parameters employed in the models.

The multi-model GSA leads to a more even level of sensitivity of PF across model parameters as compared with results for the single-model

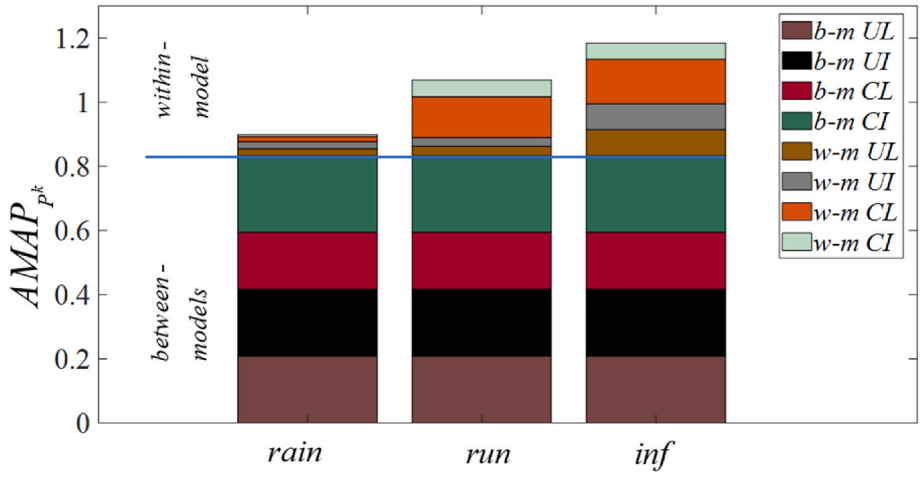

Fig. 6. Process-based sensitivity indices $AMAP_{P^k}$ for system process P^k (k = *rain*; *run*; *inf*). The *between-models* (b–m) and *within-model* (w–m) terms are also highlighted for each process.

GSA. Within the multi-model context, we find that the *between-models* contribution is key to the degree of sensitivity of PF to each parameter. This is due to the observed differences in the values of PF obtained when diverse hyetograph models are adopted. The process based analysis confirms the relevance of the *between-models* contribution in our setting. Uncertainty in the assessment of PF is mainly driven by the infiltration process, followed by the runoff and the intensity of the rain event.

Our work highlights the importance of incorporating the uncertainty arising from the lack of deterministic knowledge about not only model parameters but also model formulation when conducting a GSA of infiltration structures in urban contexts of the kind we consider. Neglecting model uncertainty (i.e., considering only a single-model context) can lead to (*a*) overconfidence on the structure performance (as rendered, e.g., through low values of PF, see Fig. 4a–b), or (*b*) excess of distrust (e.g., PF can be overestimated, see Fig. 4c-d), resulting in an oversizing of the infiltration structure (and an unnecessary cost increase) to reduce PF to acceptable limits.

CRediT authorship contribution statement

Aronne Dell'Oca: Methodology, Investigation, Formal analysis, Writing – original draft. **Alberto Guadagnini:** Conceptualization, Methodology, Writing – review & editing. **Monica Riva:** Conceptualization, Methodology, Writing – review & editing.

Declaration of competing interest

The authors declare that they have no known competing financial interests or personal relationships that could have appeared to influence the work reported in this paper.

Data availability

Data will be made available on request.

Acknowledgments

Project funded under the National Recovery and Resilience Plan (NRRP), Mission 4 Component 2 Investment 1.4 - Call for tender No. 3138 of December 16, 2021, rectified by Decree n.3175 of December 18, 2021 of Italian Ministry of University and Research funded by the European Union – NextGenerationEU; Project code CN_00000033, Concession Decree No. 1034 of June 17, 2022 adopted by the Italian Ministry of University and Research, CUP D43C22001250001, Project title "National Biodiversity Future Center - NBFC". Aronne Dell'Oca acknowledges funding from the European Union's Horizon 2020 research and innovation program under the Marie Sklodowska-Curie [Grant Agreement No. 895152, MixUQ].

References

Ahiablame, L.M., Engel, B.A., Chaubey, I., 2013. Effectiveness of low impact development practices in two urbanized watersheds: retrofitting with rain barrel/cistern and porous pavement. J. Environ. Manag. 119, 151–161. https://doi.org/10.1016/j.jenvman.2013.01.019.

Ahiablame, L., Shakya, R., 2016. Modeling flood reduction effects of low impact development at a watershed scale. J. Environ. Manag. 171, 81–91. https://doi.org/10.1016/j.jenvman.2016.01.036.

Akan, A.O., 2002. Sizing stormwater infiltration structures. J. Hydrol. Eng. 128 (5), 534–537. https://doi.org/10.1061/(ASCE)0733-9429(2002)128:5(534).

Azizian, A., 2018. Uncertainty analysis of time of concentration equations based on first-order-analysis (FOA) method. Am. J. Eng. Appl. Sci. 11 (1), 327–341. https://doi.org/10.3844/ajeassp.2018.327.341.

Bach, P.M., Rauch, W., Mikkelsen, P.S., McCarthy, D.T., Deletic, A., 2014. A critical review of integrated urban water modelling-Urban drainage and beyond. Environ. Model. Software 54, 88–107. https://doi.org/10.1016/j.envsoft.2013.12.018.

Baek, S.-S., Choi, D.-H., Jung, J.-W., Lee, H.-J., Lee, H., Yoon, K.-S., Cho, K.H., 2015. Optimizing low impact development (LID) for stormwater runoff treatment in urban area, Korea: experimental and modeling approach. Water Res. 86, 122–131. https://doi.org/10.1016/j.watres.2015.08.038.

Ballinas-González, H.A., Alcocer-Yamanaka, V.H., Canto-Rios, J.J., Simuta-Champo, R., 2020. Sensitivity analysis of the rainfall–runoff modeling parameters in data-scarce urban catchment. Hydrol. 7, 73. https://doi.org/10.3390/hydrology7040073.

Beven, K., 2006. A manifesto for the equifinality thesis. J. Hydrol. 320, 18–36. https://doi.org/10.1016/j.jhydrol.2005.07.007.

Bianchi Janetti, E., Guadagnini, L., Riva, M., Guadagnini, A., 2019. Global sensitivity analyses of multiple conceptual models with uncertain parameters driving groundwater flow in a regional-scale sedimentary aquifer. J. Hydrol. 574, 544–556. https://doi.org/10.1016/j.jhydrol.2019.04.035.

Blöschl, G., et al., 2019. Twenty-three unsolved problems in hydrology (UPH) - a community perspective. Hydrol. Sci. J. 64 (10), 1141–1158. https://doi.org/10.1080/02626667.2019.1620507.

Bouwer, H., 1969. Infiltration of water into nonuniform soil. J. Irrigat. Drain. Eng. 95, 451–462. https://doi.org/10.1061/JRCEA4.0000669.

Braswell, A.S., Ryan, J., Winston Hunt, W.F., 2018. Hydrologic and water quality performance of permeable pavement with internal water storage over a clay soil in Durham, North Carolina. J. Environ. Manag. 224, 277–287. https://doi.org/10.1016/j.jenvman.2018.07.040.

Bredehoeft, J.D., 2005. The conceptualization model problem-surprise. Hydrogeol. J. 13, 37–46. https://doi.org/10.1007/s10040-004-0430-5.

Brunetti, G., Šimůnek, J., Turco, M., Piro, P., 2018. On the use of global sensitivity analysis for the numerical analysis of permeable pavements. Urban Water J. 15 (3), 269–275. https://doi.org/10.1080/1573062X.2018.1439975.

Burlando, P., Rosso, R., 1996. Scaling and multiscaling models of depth-duration-frequency curves for storm precipitation. J. Hydrol. 187, 45–64. https://doi.org/10.1016/S0022-1694(96)03086-7.

Burnham, K.P., Anderson, A.R., 2002. Model Selection and Multiple Model Inference: A Practical Information-theoretical Approach, second ed. Springer, New York. https://doi.org/10.1007/b97636.

Busker, T., de Moel, H., Haer, T., Schmeits, M., van den Hurk, B., Myers, K., Cirkel, D.G., Aerts, J., 2022. Blue-green roofs with forecast-based operation to reduce the impact of weather extremes. J. Environ. Manag. 301, 113750 https://doi.org/10.1016/j.jenvman.2021.113750.

Buytaert, W., De Bièvre, B., Wyseure, G., Deckers, J., 2004. The use of the linear reservoir concept to quantify the impact of changes in land use on the hydrology of catchments in the Andes. Hydrol. Earth Syst. Sci. 8 (1), 108–114. https://doi.org/10.5194/hess-8-108-2004.

Cea, L., Costabile, P., 2022. Flood risk in urban areas: modelling, management and adaptation to climate change. A Review. Hydrol. 9, 50. https://doi.org/10.3390/hydrology9030050.

Chaffin, B.C., Shuster, W.D., Garmestani, A.S., Furio, B., Albro, S.L., Gardiner, M., Spring, M., Green, O.O., 2016. A tale of two rain gardens: barriers and bridges to adaptive management of urban stormwater in Cleveland, Ohio. J. Environ. Manag. 183, 31–441. https://doi.org/10.1016/j.jenvman.2016.06.025. Part 2.

Clark, M.P., Slater, A.G., Rupp, D.E., Woods, R.A., Vrugt, J.A., Gupta, H.V., et al., 2008. Framework for Understanding Structural Errors (FUSE): a modular framework to diagnose differences between hydrological models. Water Resour. Res. 44 (12) https://doi.org/10.1029/2007WR006735.

Coles, S., 2001. An Introduction to Statistical Modeling of Extreme Values. Springer, London. https://doi.org/10.1007/978-1-4471-3675-0.

Courdent, V., Grum, M., Munk-Nielsen, T., Mikkelsen, P.S., 2017. A gain-loss framework based on ensemble flow forecasts to switch the urban drainage-wastewater system management towards energy optimization during dry periods. Hydrol. Earth Syst. Sci. 21 (5), 2531–2544. https://hess.copernicus.org/articles/21/2531/2017.

Dai, H., Ye, M., 2015. Variance-based global sensitivity analysis for multiple scenarios and models with implementation using sparse grid collocation. J. Hydrol. 528, 286–300. https://doi.org/10.1016/j.jhydrol.2015.06.034.

Dai, H., Ye, M., Walker, A.P., Chen, X., 2017. A new process sensitivity index to identify important system processes under process model and parametric uncertainty. Water Resour. Res. 53, 3476–3490. https://doi.org/10.1002/2016WR019715.

Dai, H., Zhang, F., Ye, M., Guadagnini, A., Liu, Q., Hu, B., Yuan, S., 2022. A computationally efficient method for estimating multi-model process sensitivity index. Water Resour. Res. 58, e2022WR033263 https://doi.org/10.1029/2022WR033263.

Darnthamrongkul, W., Mozingo, L.A., 2021. Toward sustainable stormwater management: understanding public appreciation and recognition of urban low impact development (LID) in the san francisco bay area. J. Environ. Manag. 300, 113716 https://doi.org/10.1016/j.jenvman.2021.113716.

Del Giudice, D., Reichert, P., Bareš, V., Albert, C., Rieckermann, J., 2015. Model bias and complexity - understanding the effects of structural deficits and input errors on runoff predictions. Environ. Model. Software 64, 205–214. https://doi.org/10.1016/j.envsoft.2014.11.006.

Dell, T., Razzaghmanesh, M., Sharvelle, S., Arabi, M., 2021. Development and application of a SWMM-based simulation model for municipal scale hydrologic assessments. Water 13, 1644. https://doi.org/10.3390/w13121644.

Dell'Oca, A., Riva, M., Guadagnini, A., 2020. Global sensitivity analysis for multiple interpretive models with uncertain parameters. Water Resour. Res. 56, e2019ER025754 https://doi.org/10.1029/2019WR025754.

Dell'Oca, A., Riva, M., Guadagnini, A., 2017. Moment-based metrics for global sensitivity analysis of hydrological systems. Hydrol. Earth Syst. Sci. 21, 6219–6234. https://doi.org/10.5194/hess-21-6219-2017.

Demuzere, M., Orru, K., Heidrich, O., Olazabal, E., Geneletti, D., Orru, H., Bhave, A.G., Mittal, N., Feliu, E., Faehnle, M., 2014. Mitigating and adapting to climate change: multi-functional and multi-scale assessment of green urban infrastructure. J. Environ. Manag. 146, 107–115. https://doi.org/10.1016/j.jenvman.2014.07.025.

Dietz, M.E., 2007. Low impact development practices: a review of current research and recommendations for future directions. Water Air Soil Pollut. 186, 351–363. https://doi.org/10.1007/s11270-007-9484-z.
Eaton, T.T., 2018. Approach and case-study of green infrastructure screening analysis for urban stormwater control. J. Environ. Manag. 209, 495–504.
Emerson, C.H., Wadzuk, B.M., Traver, R.G., 2010. Hydraulic evolution and total suspended solids capture of an infiltration trench. Hydrol. Proced. 24 (8), 1008–1014. https://doi.org/10.1002/hyp.7539.
Fatone, F., Szeląg, B., Kiczko, A., Majerek, D., Majewska, M., Drewnowski, J., Łagód, 2021. Advanced sensitivity analysis of the impact of the temporal distribution and intensity of rainfall on hydrograph parameters in urban catchments. Hydrol. Earth Syst. Sci. 25, 5493–5516.
Gao, Z., Zhang, Q.H., Xie, Y.D., Wang, Q., Dzakpasu, M., Xiong, J.Q., Wang, X.C., 2022. A novel multi-objective optimization framework for urban green-gray infrastructure implementation under impacts of climate change. Sci. Total Environ. 825, 153954 https://doi.org/10.1016/j.scitotenv.2022.153954.
Georgakakos, K.P., Seo, D.-J., Gupta, H., Schaake, J., Butts, M.B., 2004. Towards the characterization of streamflow simulation uncertainty through multimodel ensembles. J. Hydrol. 298 (1–4), 222–241. https://doi.org/10.1016/j.jhydrol.2004.03.037.
Gupta, V.K., Waymire, E., 1990. Multiscaling properties of spatial rainfall and river flow distributions. J. Geophys. Res. D 95, 1999–2009. https://doi.org/10.1029/JD095iD03p01999.
Hashemi, M., Mahjouri, N., 2022. Global sensitivity analysis-based design of low impact development practices for urban runoff management under uncertainty. Water Resour. Manag. 36, 2953–2972. https://doi.org/10.1007/s11269-022-03140-1.
Hong, Y., Liao, Q., Bonhomme, C., Chebbo, G., 2019. Physically-based urban stormwater quality modelling: an efficient approach for calibration and sensitivity analysis. J. Environ. Manag. 246, 462–471. https://doi.org/10.1016/j.jenvman.2019.06.003.
Höge, M., Guthke, A., Nowak, W., 2019. The hydrologist's guide to Bayesian model selection, averaging and combination. J. Hydrol. 572, 96–107. https://doi.org/10.1016/j.jhydrol.2019.01.072.
Hosseinzadehtalaei, P., Tabari, H., Willems, P., 2020. Climate change impact on short-duration-frequency curves over Europe. J. Hydrol. 590, 125259 https://doi.org/10.1016/j.jhydrol.2020.125249.
Hu, M., Sayama, T., Zhang, X., Tanaka, K., Takara, K., Yang, H., 2017. Evaluation of low impact development approach for mitigating flood inundation at a watershed scale in China. J. Environ. Manag. 193, 430–438. https://doi.org/10.1016/j.jenvman.2017.02.020.
IPCC, 2013. In: Stocker, T.F., Qin, D., Plattner, G.-K., Tignor, M., Allen, S.K., Boschung, J., Nauels, A., Xia, Y., Bex, V., Midgley, P.M. (Eds.), Climate Change, 2013. The Physical Science Basis. Contribution of Working Group I to the Fifth Assessment Report of the Intergovernmental Panel on Climate Change. Cambridge University Press, Cambridge, United Kingdom and New York, NY, USA, p. 1535. https://doi.org/10.1017/CBO9781107415324.
Jia, H., Yao, H., Tang, Y., Yu, S.L., Field, R., Tafuri, A.N., 2015. LID-BMPs planning for urban runoff control and the case study in China. J. Environ. Manag. 149, 65–76. https://doi.org/10.1016/j.jenvman.2014.10.003.
Koc, K., Ekmekcioğlu, Ö., Özger, M., 2021. An integrated framework for the comprehensive evaluation of low impact development strategies. J. Environ. Manag. 294, 113023 https://doi.org/10.1016/j.jenvman.2021.113023.
Kourtis, I.M., Tsihrintzis, V.A., 2022. Update of intensity-duration-frequency (IDF) curves under climate change: a review. Water Supply 22 (5), 4952. https://doi.org/10.2166/ws.2022.152.
La Cecilia, D., Porta, G.M., Tang, F.H.M., Riva, M., Maggi, F., 2020. Probabilistic indicators for soil and groundwater contamination risk assessment. Ecol. Indicat. 115, 1006424 https://doi.org/10.1016/j.ecolind.2020.106424.
Larsen, A.N., Gregersen, I.B., Christensen, O.B., Linde, J.J., Mikkelsen, P.S., 2009. Potential future increase in extreme one-hour precipitation events over Europe due to climate change. Water Sci. Technol. 60, 9. https://doi.org/10.2166/wst.2009.650.
Lee, S., Qi, J., McCarty, G.W., Yeo, I.-Y., Zhang, X., Moglen, G.E., Du, L., 2021. Uncertainty assessment of multi-parameter, multi-GCM, and multi-RCP simulations for streamflow and non-floodplain wetland (NFW) water storage. J. Hydrol. 600, 126564 https://doi.org/10.1016/j.jhydrol.2021.126564.
Leimgruber, J., Krebs, G., Camhy, D., Muschalla, D., 2018. Sensitivity of model-based water balance to low impact development parameters. Water 10 (1838), 1–19. https://doi.org/10.3390/w10121838.
Li, Q., Wang, F., Yu, Y., Huang, Z., Li, M., Guan, Y., 2019. Comprehensive performance evaluation of LID practices for the sponge city construction: a case study in Guangxi, China. J. Environ. Manag. 231, 10–20. https://doi.org/10.1016/j.jenvman.2018.10.024.
Li, S., Wang, Z., Wu, X., Zeng, Z., Lai, C., 2022. A novel spatial optimization approach for the cost-effectiveness improvement of LID practices based on SWMM-FTC. J. Environ. Manag. 307, 114574 https://doi.org/10.1016/j.jenvman.2022.114574.
Li, J., Zhao, R., Li, Y., Chen, L., 2018. Modeling the effects of parameter optimization on three bioretention tanks using the HYDRUS-1D model. J. Environ. Manag. 217, 38–46. https://doi.org/10.1016/j.jenvman.2018.03.078.
Liao, D., Zhang, Q., Wang, Y., Zhu, H., Sun, J., 2021. Study of four rainstorm design methods in chongqing. Front. Environ. Sci. 9, 639931 https://doi.org/10.3389/fenvs.2021.639931.
Lima, C.H.R., Kwon, H.H., Kim, Y.T., 2018. A local-regional scaling invariant Bayesian GEV model for estimating rainfall IDF curves in future climate. J. Hydrol. 566, 73–88. https://doi.org/10.1016/j.jhydrol.2018.08.075.
Liu, Y., Chaubey, I., Bowling, L.C., 2016. Sensitivity and Uncertainty Analysis of the L-THIA-LID 2.1 Model. Water Resour. Manage., pp. 4927–4949. https://doi.org/10.1007/s11269-016-1462-z
Locatelli, L., Mark, O., Mikkelsen, P.S., Arnbjerg-Nielsen, K., Wong, T., Binning, P.J., 2015. Determining the extent of groundwater interference on the performance of infiltration trenches. J. Hydrol. 529 (3), 1360–1372. https://doi.org/10.1016/j.jhydrol.2015.08.047.
Madrazo-Uribeetxebarria, E., Antín, M.G., Berrondo, J.A., Andrés-Doménech, I., 2021. Sensitivity analysis of permeable pavement hydrological modelling in the Storm Water Management Model. J. Hydrol. 600, 126525 https://doi.org/10.1016/j.jhydrol.2021.126525.
Mei, C., Liu, J., Wang, H., Yang, Z., Ding, X., Shao, W., 2018. Integrated assessments of green infrastructure for flood mitigation to support robust decision-making for sponge city construction in an urbanized watershed. Sci. Total Environ. 639, 1394–1407. https://doi.org/10.1016/j.scitotenv.2018.05.199.
Morris, M.D., 1991. Factorial sampling plans for preliminary computational experiments. Technometrics 33 (2), 161–174. https://doi.org/10.1080/00401706.1991.10484804.
Naves, J., Rieckermann, J., Cea, L., Puertas, J., Anta, J., 2020. Global and local sensitivity analysis to improve the understanding of physically-based urban wash-off models from high-resolution laboratory experiments. Sci. Total Environ. 709, 136152 https://doi.org/10.1016/j.scitotenv.2019.136152.
Neuman, S.P., 2003. Maximum likelihood Bayesian averaging of alternative conceptual-mathematical models. Stoch. Environ. Res. Risk Assess. 17 (5), 291–305. https://doi.org/10.1007/s00477-003-0151-7.
Pianosi, F., Beven, K., Freer, J., Hall, J.W., Rougier, J., Stephenson, D.B., Wagener, T., 2016. Sensitivity analysis of environmental models: a systematic review with practical workflow. Environ. Model. Software 79, 214–232. https://doi.org/10.1016/j.envsoft.2016.02.008.
Poeter, E.P., Anderson, D.A., 2005. Multimodel ranking and inference in ground water modeling. Ground Water 43 (4), 597–605. https://doi.org/10.1111/j.1745-6584.2005.0061.x.
Poeter, E.P., Hill, M.C., 2007. MMA: a computer code for multi-model analysis. In: United States Geological Survey, Technology & Methods, 6-E3. USGS, Reston, Va, p. 113. https://doi.org/10.3133/tm6E.
Pour, S.H., Wahab, A.K.A., Shahid, S., Asaduzzaman, M., Dewan, A., 2020. Low impact development techniques to mitigate the impacts of climate-change-induced urban floods: current trends, issues and challenges. Sustain. Cities Soc. 62, 102373 https://doi.org/10.1016/j.scs.2020.102373.
Pumo, D., Francipane, A., Alongi, F., Noto, L.V., 2023. The potential of multilayer green roofs for stormwater management in urban area under semi-arid Mediterranean climate conditions. J. Environ. Manag. 326, 116643 https://doi.org/10.1016/j.jenvman.2022.116643. Part A.
Qin, H.-P., Li, Z.-X., Fu, G., 2013. The effects of low impact development on urban flooding under different rainfall characteristics. J. Environ. Manag. 129, 577–585. https://doi.org/10.1016/j.jenvman.2013.08.026.
Radinja, M., Škerjanec, M., Šraj, M., Džeroski, S., Todorovski, L., Atanasova, N., 2021. Automated modelling of urban runoff based on domain knowledge and equation discovery. J. Hydrol. 603, 127077 https://doi.org/10.1016/j.jhydrol.2021.127077. Part C.
Ragno, E., AghaKouchak, A., Love, C.A., Cheng, L., Vahedifard, F., Lima, C.H.R., 2018. Quantifying changes in future intensity-duration-frequency curves using multimodel ensemble simulations. Water Resour. Res. 54, 3. https://doi.org/10.1002/2017WR021975.
Ravazzani, G., Boscarello, L., Cislaghi, A., Mancini, M., 2019. Review of time of concentration equation and a new proposal in Italy. J. Hydrol. Engineer. 24 (10), 04019039 https://doi.org/10.1061/(ASCE)HE.1943-5584.0001818.
Razavi, S., Gupta, H.V., 2016. A new framework for comprehensive, robust, and efficient global sensitivity analysis: 1. Theory. Water Resour. Res. 52 (1), 423–439.
Razavi, S., Jakeman, A., Saltelli, A., Prieur, C., Iooss, B., Borgonovo, B., Plischke, E., Lo Piano, S., Iwanaga, T., Becker, W., Tarantola, S., Guillaume, J.H.A., Jakeman, J., Gupta, H., Melillo, N., Rabitti, G., Chabridon, V., Duan, Q., Sun, X., Smith, S., Sheikholeslami, R., Hosseini, N., Asadzadeh, M., Puy, A., Kucherenko, S., Maier, H. R., 2021. The Future of Sensitivity Analysis: an essential discipline for systems modeling and policy support. Environ. Model. Software 137, 104954. https://doi.org/10.1016/j.envsoft.2020.104954.
Recanatesi, F., Petroselli, A., Ripa, M.N., Leone, A., 2017. Assessment of stormwater runoff management practices and BMPs under soil sealing: a study case in a peri-urban watershed of the metropolitan area of Rome (Italy). J. Environ. Manag. 201, 6–18. https://doi.org/10.1016/j.jenvman.2017.06.024.
Riva, M., Mambretti, S., Chaynikov, S., Ackerer, P., Fasunwon, O., Guadagnini, A., 2013. A new general analytical solution for infiltration structures design. J. Hydraul. Engineer. 139 (6), 637–644. https://doi.org/10.1061/(ASCE)HY.1943-7900.0000718.
Roldin, M., Locatelli, L., Mark, O., Mikkelsen, P.S., Binning, P.J., 2013. A simplified model of a soafaway infiltration interaction with a shallow groundwater table. J. Hydrol. 497, 165–175. https://doi.org/10.1016/j.jhydrol.2013.06.005.
Rong, Q., Liu, Q., Xu, C., Yue, W., Su, M., 2022. Optimal configuration of low impact development practices for the management of urban runoff pollution under uncertainty. J. Environ. Manag. 320, 115821 https://doi.org/10.1016/j.jenvman.2022.115821.
Saadatpour, M., Delkhosh, F., Afshar, A., Solis, S.S., 2020. Developing a simulation-optimization approach to allocate low impact development practices for managing hydrological alterations in urban watershed. Sustain. Cities Soc. 61, 102334 https://doi.org/10.1016/j.scs.2020.102334.

Saavedra, D., Mendoza, P.A., Addor, N., Llauca, H., Vargas, X., 2022. A multi-objective approach to select hydrological models and constrain structural uncertainties for climate impact assessments. Hydrol. Process. 36 (1), e14446 https://doi.org/10.1002/hyp.14446.

Saurav, K.C., Shrestha, S., Ninsawat, S., Chonwattana, S., 2021. Predicting flood events in Kathmandu Metropolitan City under climate change and urbanisation. J. Environ. Manag. 281, 111894 https://doi.org/10.1016/j.jenvman.2020.111894.

Semadeni-Davies, A., Hernebring, C., Svensson, G., Gustafsson, L.-G., 2008. The impacts of climate change and urbanisation on drainage in Helsingborg, Sweden: suburban stormwater. J. Hydrol. 350 (1–2), 114–125. https://doi.org/10.1016/j.jhydrol.2007.11.006.

Sieker, F., 1984. Stormwater infiltration in urban areas. In: Proceedings of the Third International Conference on Urban Storm Drainage (Goteborg).

Sikorska, A.E., Scheidegger, A., Banasik, K., Rieckermann, J., 2012. Bayesian uncertainty assessment of flood predictions in ungauged urban basins for conceptual rainfall-runoff models. Hydrol. Earth Syst. Sci. 16 (4), 1221–1236. https://hess.copernicus.org/articles/16/1221/2012/.

Sobol, I.M., 1993. Sensitivity analysis for non-linear mathematical models. Mathem. Model. Computat. Experim. 1, 407–414.

Sohn, W., Kim, J.-H., Li, M.-H., Brown, R., 2019. The influence of climate on the effectiveness of low impact development: a systematic review. J. Environ. Manag. 236, 365–379. https://doi.org/10.1016/j.jenvman.2018.11.041.

Song, J.-Y., Chung, E.-S., Kim, S.H., 2018. Decision support system for the design and planning of low-impact development practices: the case of seoul. Water 10, 146. https://doi.org/10.3390/w10020146.

Sui, X., van de Ven, F.H.M., 2023. The influence of Low Impact Development (LID) on basin runoff in a half-urbanized catchment: a case study in San Antonio, Texas. J. Hydrol. 616, 128793 https://doi.org/10.1016/j.jhydrol.2022.128793.

Tellman, B., Sullivan, J.A., Kuhn, C., Kettner, A.J., Doyle, C.S., Brakenridge, G.R., Erickson, T.A., Slayback, D.A., 2021. Satellite imaging reveals increased proportion of population exposed to floods. Nature 596, 80–86. https://doi.org/10.1038/s41586-021-03695-w.

Tirpak, R.A., Hathaway, J.M., Khojandi, A., Weathers, M., Epps, T.H., 2021. Building resiliency to climate change uncertainty through bioretention design modifications. J. Environ. Manag. 287, 112300 https://doi.org/10.1016/j.jenvman.2021.112300.

Tscheikner-Gratl, F., Bellos, V., Schellart, A., Moreno-Rodenas, A., Muthusamy, M., Langeveld, J., Clemens, F., Benedetti, L., Rico-Ramirez, M.A., de Carvalho, R.F., Breuer, L., Shucksmith, J., Heuvelink, G.B.M., Tait, S., 2019. Recent insights on uncertainties present in integrated catchment water quality modelling. Water Res. 150, 368–379. https://doi.org/10.1016/j.watres.2018.11.079.

Todeschini, S., Papiri, S., Ciaponi, C., 2012. Performance of stormwater detention tanks for urban drainage systems in northern Italy. J. Environ. Manag. 101, 33–45. https://doi.org/10.1016/j.jenvman.2012.02.003.

Troin, M., Martel, J.-L., Arsenault, R., Brissette, F., 2022. Large-sample study of uncertainty of hydrological model components over North America. J. Hydrol. 609, 127766 https://doi.org/10.1016/j.jhydrol.2022.127766.

Ventura, G., 1905. Bonificazione della Bassa pianura bolognese: studio sui coefficienti udometrici. Giornale del Genio Civile 43 (3), 3–36.

Wang, F., Huang, G., Cheng, G., Li, Y., 2021. Multi-level factorial analysis for ensemble data-driven hydrological prediction. Adv. Water Resour. 153, 103948 https://doi.org/10.1016/j.advwatres.2021.103948.

Wang, X.Q., Huang, G.H., Liu, J.L., 2014. Projected increases in intensity and frequency of rainfall extremes through a regional climate modeling approach. J. Geophys. Res. Atmos. 119 (23), 13–271. https://doi.org/10.1002/2014jd022564.

Wang, M., Sun, X., Sweetapple, C., 2017. Optimization of storage tank locations in an urban stormwater drainage system using a two-stage approach. J. Environ. Manag. 204 (1), 31–38. https://doi.org/10.1016/j.jenvman.2017.08.024.

Wang, M., Zhang, D.Q., Su, J., Dong, J.W., Tan, S.K., 2018. Assessing hydrological effects and performance of low impact development practices based on future scenarios modeling. J. Clean. Prod. 179, 12–23. https://doi.org/10.1016/j.jclepro.2018.01.096.

Whling, T., Vrugt, J.A., 2008. Combining multiobjective optimization and Bayesian model averaging to calibrate forecast ensembles of soil hydraulic models. Water Resour. Res. 44 (12), W12432 https://doi.org/10.1029/2008WR007154.

Winsemius, H.C., Aerts, J.C.J.H., van Beek, L.P.H., Bierkens, M.F.P., Bouwman, A., Jongman, B., Kwadijk, J.C.J., Ligtvoet, W., Lucas, P.L., van Vuuren, D.P., Ward, P.J., 2015. Global drivers of future river flood risk. Nat. Clim. Change 6, 381.

Woods-Ballard, B., Kellargher, R., Martin, P., Jefferies, C., Bray, R., Shaffer, P., 2007. The SuDS Manual C695. Construction Industry Research and Information Association (CIRIA), London.

Xu, T., Li, K., Engel, B.A., Jia, H., Leng, L., Sun, Z., Yu, S.L., 2019a. Optimal adaptation pathway for sustainable low impact development planning under deep uncertainty of climate change: a greedy strategy. J. Environ. Manag. 248, 109280 https://doi.org/10.1016/j.jenvman.2019.109280.

Xu, Z., Xiong, L., Li, H., Xu, J., Cai, X., Chen, K., Wu, J., 2019b. Runoff simulation of two typical urban green land types with the Stormwater Management Model (SWMM): sensitivity analysis and calibration of runoff parameters. Environ. Monit. Assess. 191, 343. https://doi.org/10.1007/s10661-019-7445-9.

Yang, W., Wang, Z., Hua, P., Zhang, J., Krebs, P., 2021. Impact of green infrastructure on the mitigation of road-deposited sediment induced stormwater pollution. Sci. Total Environ. 770, 145294 https://doi.org/10.1016/j.scitotenv.2021.145294.

Yang, J., Ye, M., 2022. A new multi-model absolute difference-based sensitivity (MMADS) analysis method to screen non-influential processes under process model and parametric uncertainty. J. Hydrol. 608, 127609 https://doi.org/10.1016/j.jhydrol.2022.127609.

Yao, L., Wu, Z., Wang, Y., Sun, S., Wei, W., Xu, Y., 2020. Does the spatial location of green roofs affects runoff mitigation in small urbanized catchments? J. Environ. Manag. 268, 110707 https://doi.org/10.1016/j.jenvman.2020.110707.

Ye, M., Neuman, S.P., Meyer, P.D., 2004. Maximum likelihood Bayesian averaging of spatial variability models in unsaturated fractured tuff. Water Resour. Res. 40 (5), W05113 https://doi.org/10.1029/2003WR002557.

Ye, M., Meyer, P.D., Neuman, S.P., 2008. On model selection criteria in multimodel analysis. Water Resour. Res. 44 (3), W03428 https://doi.org/10.1029/2008WR006803.

Yeo, M.H., Nguyen, V.T.V., Kpodonu, T.A., 2021. Characterizing extreme rainfalls and constructing confidence intervals for IDF curves using Scaling - GEV distribution models. Int. J. Climatol. 41, 456–468. https://doi.org/10.1002/joc.6631.

Zakizadeh, F., Moghaddam, N.A., Salajegheh, A., Sañudo-Fontaneda, L.A., Alamdari, N., 2022. Efficient urban runoff quantity and quality modelling using SWMM model and field data in an urban watershed of Tehran metropolis. Sustainability 14, 1086. https://doi.org/10.3390/su14031086.

Zeng, S., Guo, H., Dong, X., 2019. Understanding the synergistic effect between LID facility and drainage network: with a comprehensive perspective. J. Environ. Manag. 246, 849–859. https://doi.org/10.1016/j.jenvman.2019.06.028.

Zhang, K., Manuelpillai, D., Raut, B., Deletic, A., Bach, P.M., 2019. Evaluating the reliability of stormwater treatment systems under various future climate conditions. J. Hydrol. 568, 57–66. https://doi.org/10.1016/j.jhydrol.2018.10.056.

Zischg, J., Zeisl, P., Winkler, D., Rauch, W., Sitzenfrei, R., 2018. On the sensitivity of geospatial low impact development locations to the centralized sewer network. Water Sci. Technol. 77 (7), 1851–1860. https://doi.org/10.2166/wst.2018.060.

Zhu, Z., Chen, Z., Chen, X., Yu, G., 2019. An assessment of the hydrologic effectiveness of low impact development (LID) practices for managing runoff with different objectives. J. Environ. Manag. 231, 504–514. https://doi.org/10.1016/j.jenvman.2018.10.046.